Bulletin of Electrical Engineering and Informatics
Vol. 9, No. 5, October 2020, pp. 1861~1872
ISSN: 2302-9285, DOI: 10.11591/eei.v9i5.1778

Linear and nonlinear controllers of a solar photovoltaic water pumping system

M. Madark, A. Ba-razzouk, E. Abdelmounim, M. El Malah
System Analysis and Information Processing Laboratory
Science and Technical Faculty, Hassan 1st University, Settat, Morocco

Article Info

Article history:

Received Sep 4, 2019
Revised Oct 12, 2019
Accepted Mar 23, 2020

Keywords:

Backstepping control
Centrifugal pump
Induction motor
IRFOC
Lyapunov functions
MPPT
P&O
PV system
Slinding mode control
Water pumping system

ABSTRACT

This paper provided a comparative study between linear and nonlinear controllers of a solar photovoltaic (PV) water pumping system using an induction motor and a centrifugal pump. For linear controller, classical Perturb and Observe was selected to ensure the operation of the PV system at the maximum power point (MPP) and is combined with Indirect Rotor Field Oriented Control (IRFOC) based on a conventional proportional integral speed regulator chosen to control and to optimize the rotor speed. In second and third controllers, Backstepping and first order sliding mode controls were proposed for controlling the whole system. To regulate and optimize rotor speed in the nonlinear controller, all considered control techniques were combined with IRFOC in order to establish easy control laws. In addition, MPP was tracked by acting on the DC-DC converter and using its mathematical model for developing control laws. Maximum delivered power was used as reference signal for optimizing actual rotor speed. The controlled system is operated without mechanical sensors. Estimators of rotor speed and load torque were proposed based on the mathematical model of induction motor and centrifugal pump and using only available output measurements.. Simulation results were investigated and the effectiveness of the nonlinear proposed strategies.

Corresponding Author:

M. Madark,
Department of Applied Physics,
Science and Technical Faculty,
Hassan 1st University, Settat, Morocco.
Email: m.madark1987@gmail.com

1. INTRODUCTION

Solar photovoltaic water pumping system is a promising solution to solve the water shortage problem in Morocco. This is especially interesting in remotes areas, where the country has a considerable solar potential over 3000 hours of yearly sunshine and an incident solar radiation greater than 5 KWh/m² [1]. Furthermore, to meet its increasingly demand and to decrease its fossil fuel energy sources dependence, Morocco launched the Moroccan Solar Plan as part of its national energy strategy 2030. Due to this strategy, 35 percent of its electricity from renewable energy sources had been produced in 2018 and it aims to produce 52 percent by 2030. In the next ten years, the Kingdom has a plan to massively exploit this clean and intermittent energy and to reduce its energy dependence on foreign countries, from 95% to 85% by 2020. Solar photovoltaic energy offers an advantageous and competitive alternative compared to other traditional energy resources. According to Moroccan Agency for Energy Efficiency, these systems remain the cheapest energy sources and diesel is the most expensive energy sources [2]. Today, characteristics of economic growth based on the consumption of oil are measured in terms of ethics. Regarding this non-renewable fossil

resource, it took several hundred million years to produce it and only a few decades to exhaust it. If we add fossil fuel depletion and climate change, then we measure how much the energy transition is necessary and even urgent. The development of renewable sources is essential, with an associated absolute priority. The use of conventional oil energy in pumping system can disturb the livestock, pollute the agriculture environment and require transportation that increases the cost of its exploitation. These significant drawbacks lead to the study of the control of solar photovoltaic water pumping system (SPVWPS), which is the most important and appropriate use of photovoltaic in this paper. PV generator, boost converter, DC-link voltage, three phase voltage source inverter (VSI), squirrel cage induction motor, centrifugal pump, controller including MPPT, rotor flux orientation, rotor speed control unit, and storage tank are the main components of SPVWPS.

Energy from photovoltaic sources is intermittent and dependent on climatic conditions. Since these conditions are not favorable to provide enough energy continuously all day and during the night, the photovoltaic generators are generally coupled to the motor-pump unit through a conversion system which makes it possible to control the system by optimizing the energy produced by the generator. Therefore this energy is exploited to store water in a tank to ensure its availability all times. In addition, the generator has non-linear characteristics with maximum power points. These characteristics depend on the irradiance and the temperature level. Furthermore, depending on the characteristics of the load supplied by this generator, it is possible to find a very large difference between the potential power of the generator and that actually transferred to the load in direct connection mode. The first objective of this work is to study maximum power point tracking and thus, to transfer of the maximum power of the generator towards the motor-pump drive system by means of a boost converter. The second objective is to regulate the rotor flux level at its rated value and the mechanical speed of the induction motor at a reference deduced from the maximum power of the generator, to extract maximum water quantity, by controlling the VSI.

In recent decades, many methods for extracting MPP have been developed such as Perturb and Observe (P&O) [3-5], Incremental Inductance [3],[6], Fuzzy Logic [7-8], Artificial Neural Network [9], [10] Backstepping [11], Backstepping with Integral Action [12], First Order Sliding Mode [13]. These techniques differ in many aspects such as sensors requirements, complexity, cost, efficiency, speed of convergence, robustness of tracking during irradiation and temperature changes, and necessary equipments for digital implementation. P&O has a simple control structure and reduced number of measured parameters, however the major drawbacks of P&O algorithm are presence of oscillations around the MPP in steady state operation and occasional deviation from the maximum operating point in case of rapidly changing atmospheric conditions, such as broken clouds [14]. The control of the induction motor remain complex due to the nonlinearity of its mathematical model, high order degree, parameters variations and detuning between rotor flux and electromagnetic torque.

For these reasons, using IRFOC based on classical PI speed controller to implement a high performance induction motor drive is often characterized by an overshoot during startup, undershoot while applying loads, steady-state error on speed, oscillation in the torque response and overshoot again at load removal [15]. Induction motor vector control based on nonlinear approaches, such as Backstepping, first order sliding mode, guarantee the global asymptotic stability of the closed-loop system. In addition, these nonlinear controllers can solve problems related to classical MPPT. However, these techniques suffer from sensitivity to parameters variation, need for measuring all state variables and require observers if some state variables are not measurable. To achieve good performance, expensive mechanical sensors required in nonlinear control laws and used to measure load torque and rotor speed, are replaced using estimators. This paper is organized into five sections: mathematical model of the solar photovoltaic water pumping system are described in section II. Section III presents the proposed linear and nonlinear control schemes of the system and the developments of estimators for rotor speed, rotor flux and load torque disturbances. Section V analyses and discusses simulation results of this comparative study. Conclusions and recommendations are given in section VI.

2. SPVWPS MATHEMATICAL MODEL

Most of SPVWPS have the added advantage of storing water for use when the sun is not shining, eliminating the need for batteries, enhancing simplicity and reducing overall system costs [16]. Figure 1 illustrates solar-powered water pumping system configuration. Photovoltaic pumping system is composed of:

- A generator consisting of photovoltaic modules interconnected to form a unit of direct current production.
- A power conditioning unit, consisting of static converters (boost and inverter), capable of varying the frequency and the output voltage according to the available power of the solar generator.
- An immersed electric pump unit consisting of an induction electric motor and a centrifugal pump.
- A hydraulic infrastructure that drives water from its source to a storage tank.

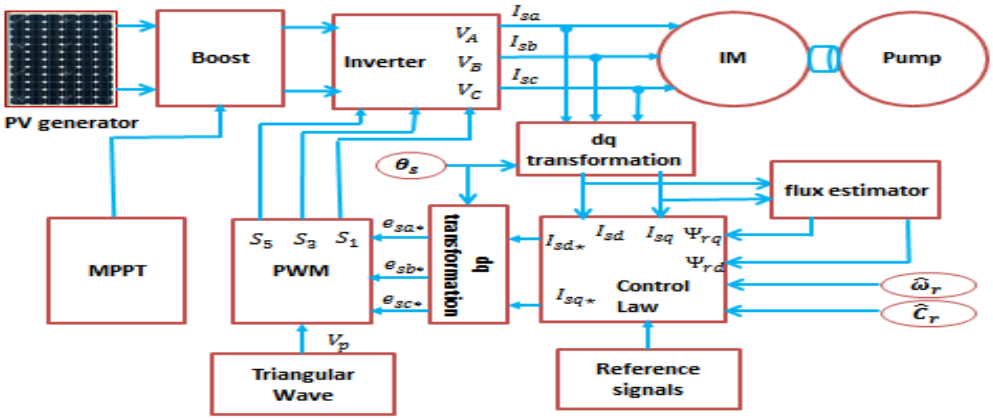

Figure 1. Solar-powered water pumping system control scheme

2.1. PV cell and PV generator mathematical model

Photovoltaic cell model necessarily involves a judicious choice of equivalent electrical circuits. Several mathematical models were developed to represent the nonlinear behaviour of the cell [16]. These models differ from each other by the mathematical procedures and the number of parameters. In this work, we have chosen PV solar-cell single diode model which is a current source in parallel with one diode and both series and parallel resistors. The single-diode model has less computation time and less number of unknown parameters [17]. Equivalent electrical circuit is reported in Figure 2.

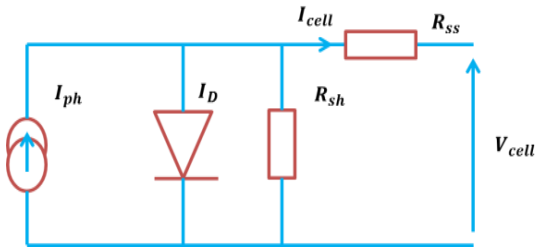

Figure 2. Equivalent electrical circuit

The following equations describes the mathematical model of the PV solar-cell

$$I_{cell} = I_{ph} - I_s\left(\exp\left(q\frac{V_{cell}+R_{ss}I_{cell}}{\gamma KT}\right)-1\right)-\frac{V_{cell}+R_{ss}I_{cell}}{R_{sh}} \quad (1)$$

$$I_{ph} = \frac{E}{E_{ref}}\left(I_{sc}+K_i\left(T-T_r\right)\right) \quad (2)$$

$$I_s = I_{rs}\left(\frac{T}{T_r}\right)^3 \exp\left(-\frac{qE_{g0}}{\gamma K}\left(\frac{1}{T}-\frac{1}{T_r}\right)\right) \quad (3)$$

Where I_{cell}, V_{cell}, I_{ph}, I_{rs}, I_{sc}, E_{ref}, E, T_r, T, K_i, q, K, R_{ss} and R_{sh} are the current across the cell, the solar cell output voltage, photo-current, reverses saturation current, Cell short-circuits current at 298°K and 1kW/m², reference solar irradiation in W/m^2, solar irradiation in W/m^2, cell's reference temperature, temperature on absolute scale, Cell's short-circuits current temperature coefficient, electron charge, Boltzmann's constant, and intrinsic series and parallel resistors of the cell respectively. PV generator consists of modules connected in series and in parallel to obtain the desired power. Each module is composed of PV cells. For the modeling of the PV field, we will therefore start from the basic element which is the PV cell. The equations, described PV generator model, are given as:

$$I_{pv} = N_p I_{cell} \quad ; \quad V_{pv} = N_s V_{cell} \tag{4}$$

Where and V_{pv} are the PV array power and the PV array voltage

With N_p being parallel combinations sets of PV cell and each set consists of N_s series-connected panels. The SM55 PV panel will be used later in the validation of simulation results. The electrical specifications of SM55 PV panel are recapitulated in Table 1. In order to analyze the behavior of the chosen photovoltaic panel and PV generator, based on the three-parameter model, we carried out a simulation in Matlab/Simulink environment. The results obtained are presented in Figures 3 and 4. Simulation is provided to obtain the I-V and P-V time histories of the solar module and PV generator for different solar irradiations and temperatures.

Table 1. Electrical specifications of SM55 PV panel

Electrical specifications	Rating Values
Maximum power rating P_{emax} (W)	55
Rated current at the MPP (A)	3.15
Rated voltage at the MPP (V)	17.4
Short circuit current I_{sc} (A)	3.45
Open circuit voltage V_{oc} (V)	21.7
Current temperature coefficient (mA/°C)	1.2
N_s	36
N_p	1

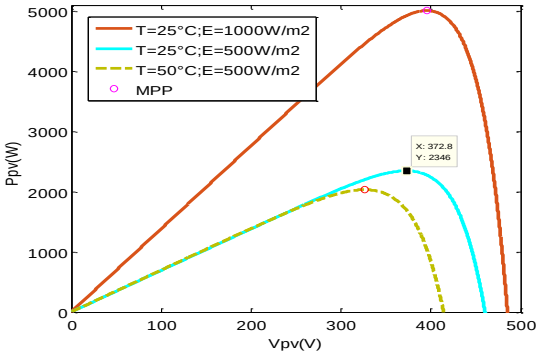

Figure 3.Ppv-Vpv Characteristics of PV generator

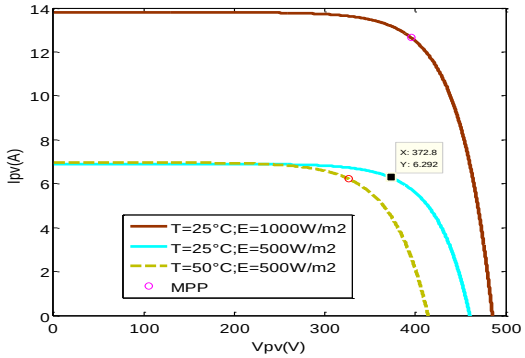

Figure 4. Ipv-Vpv Characteristics of PV generator

According to simulation results, it is possible to raise the following remarks: When the irriadiation increases the voltage and the current increases thus the power increases. In addition, when the temperature increases the current is relatively constant, however, the voltage decreases thus power decreases. Maximum power of solar module and generator depends on the value of solar irradiation and temperature. Components of MPP are summarized in the Table 2 for different values of temperature and solar irradiation. These coordinates of MPP will be used to validate the maximum power point tracker.

Table 2. Coordinates of maximum power point (MPP)

Coordinates of MPP	T (°K)	E(W/m^2)	V_{mpp} (V)	P_{mpp} (W)	I_{mpp} (A)
MPP1	298.15	1000	395.80	5007.00	12.65
MPP2	298.15	500	372.80	2346.00	6.29
MPP3	323.15	500	326.90	2032.00	6.21

2.2. Model of induction motor

Induction motor study consists of looking for all equations connecting input variables to output quantities: voltages, stator currents and torque. The different approaches for modelling IM are based on electromagnetism and mechanics equations resolution. The model of induction motor remains complex due to its high order degree, its strongest nonlinearity and the coupling between flux and torque. To simplify their electrical equations, from a six order system to four order system, a dq transformation is used. This transformation ensures instantaneous power conservation. Induction motor state space representation, expressed in synchrounsly refrence frame, is given by the following [12],[18, 19].

$$\frac{d}{dt}\begin{bmatrix}\omega_r\\ I_{sd}\\ I_{sq}\\ \Psi_{rd}\\ \Psi_{rq}\end{bmatrix}=\begin{bmatrix}a_1(\Psi_{rd}I_{sq}-\Psi_{rq}I_{sd})-a_2-a_3\omega_r\\ a_4I_{sd}+\omega_sI_{sq}+a_5\Psi_{rd}+a_6\omega_r\Psi_{rq}\\ a_4I_{sq}-\omega_sI_{sd}+a_5\Psi_{rq}-a_6\omega_r\Psi_{rd}\\ a_7I_{sd}+a_8\Psi_{rd}+(\omega_s-\omega_r)\Psi_{rq}\\ a_7I_{sq}+a_8\Psi_{rq}-(\omega_s-\omega_r)\Psi_{rd}\end{bmatrix}+\begin{bmatrix}0 & 0\\ bV_b & 0\\ 0 & bV_b\\ 0 & 0\\ 0 & 0\end{bmatrix}\begin{bmatrix}K_{sd}\\ K_{sq}\end{bmatrix} \quad (6)$$

Where:

$$a_1=\frac{3}{2}\frac{p^2\mathrm{M}}{JL_r};\quad a_2=\frac{pC_r}{J};\quad a_3=\frac{pF}{J};\quad a_4=-\frac{1}{\sigma\tau_s}+\frac{1-\sigma}{\sigma\tau_r};\quad a_5=\frac{\mathrm{M}}{\sigma L_rL_s\tau_r} \quad (7)$$

$$a_6=\frac{\mathrm{M}}{\sigma L_rL_s};\ a_7=\frac{\mathrm{M}}{\tau_r}\quad a_8=-\frac{1}{\tau_r}\quad ;\quad b=\frac{1}{\sigma L_s} \quad (8)$$

Where I_{sd}, I_{sq}, V_{sd}, V_{sq}, K_{sd}, K_{sq}, Ψ_{rd}, Ψ_{rd}, Ψ_r, ω_s, ω_r, ω_{mec}, R_s, L_s, T_{em}, C_r, M, K_f, V_{dc}, σ, p, τ_r, τ_s and R_r are dq axis stator current components, dq axis stator voltage components, input control components, dq axis rotor flux components, rotor flux, stator electric angular pulsation, rotor electric angular pulsation, mechanical speed, stator resistance, stator inductance, electromagnetic torque, load torque, mutual inductance, viscous friction coefficient, DC link voltage, leakage coefficient, number of pole pairs, rotor time-constant, stator time-constant and rotor resistance.

This complete model can be considerably simplified by considering an IM supplied by a source voltage inverter which is controlled by current supply and by using the indirect rotor field oriented control. Indeed, when the stator currents are imposed, the statorique phases dynamics can be neglected. The dynamic behavior of the machine is exclusively described by that of the rotor phases. Therefore, in this case, simplified second- order model of a current-fed induction motor used to desing simple control laws is formulated as [18]:

$$\frac{d}{dt}\begin{bmatrix}\omega_r\\ \Psi_r\end{bmatrix}=\begin{bmatrix}-a_2-a_3\omega_r\\ a_8\Psi_r\end{bmatrix}+\begin{bmatrix}0 & a_1\Psi_r\\ a_7 & 0\end{bmatrix}\begin{bmatrix}I_{sd}\\ I_{sq}\end{bmatrix} \quad (9)$$

2.3. Boost converter model

The DC-DC boost converter is an interface that allows adaptation between the PV generator and the other components of the system in order to extract maximum power. It aims to step up the input voltage and provides at output an ajdjustable DC voltage. This device contains a diode, a switch, an inductance which is added as energy storage element and a capacitor added to output to remove voltage ripple. The following state equations describe the boost converter model:

$$\begin{cases} \dfrac{dV_{pv}}{dt} = \dfrac{I_{pv} - I_L}{C_p} \\ \dfrac{dI_L}{dt} = \dfrac{V_{pv} - (1-u)V_b}{L_b} \\ \dfrac{dV_b}{dt} = \dfrac{(1-u)I_L - I_b}{C_b} \end{cases} \tag{10}$$

2.4. Voltage source inverter model

DC to AC converter is used to control rotor speed and rotor flux of the induction motor, mechanically coupled to centrifugal pump, based on the actual situation of the system. Morover, the inverter is able to adjust operating point to an optimal rotor speed deduced from the maximum power point. Assuming that the electronic devices of the inverter are ideal and the load fed by the inverter is a balanced three-phase load, it is possible to formulate the nonlinear model of this converter based only on the switching functions and the DC voltage input.

$$\begin{bmatrix} V_{AN} \\ V_{BN} \\ V_{CN} \end{bmatrix} = \frac{1}{3}\begin{bmatrix} 2 & -1 & -1 \\ -1 & 2 & -1 \\ -1 & -1 & 2 \end{bmatrix}\begin{bmatrix} K_1 \\ K_2 \\ K_3 \end{bmatrix} V_b \tag{11}$$

With K_1, K_2 and K_3 being the switching functions and V_b the voltage output of the boost converter. Output currents satisfy the following equation:

$$K_1 i_{sa} + K_2 i_{sb} + K_3 i_{sc} = 0 \tag{12}$$

With i_{sa}, i_{sb} and i_{sc} being the stator currents of induction motor.

2.5. Centrifugal pump

Centrifugal pump load torque and mechanical power can be modeled by the folloying expressions [20]:

$$C_r = K\omega_r^2 \tag{13}$$

$$P_r = K\omega_r^3 \tag{14}$$

Where C_r is the load torque and P_r is the mechanical power.

3. DESIGN LINEAR AND NONLINEAR CONTROLLERS

In this section, maximum power point tracking and inverter control will be presented using P&O algorithm to control the boost converter. In addition, IRFOC of induction motor based on classical PI speed regulator is considered, and the overall system control by two nonlinear control techniques will be discussed. Finally, load torque and rotor speed estimators will be developed.

3.1. P&O algorithm based MPPT technique

MPPT technique tracks MPP from the measured currents, voltages, or powers. It can react to unpredictable changes in PV generator operation. For this, the voltage of the operating point is incremented in regular intervals. If the output power is larger, then the direction is maintained for the next step. Otherwise it will be reversed. The actual operating point then oscillates around the MPP. P&O disturbs voltage of PV generator with ΔV and observes its PV power variation at the output [21-24]. Figures 5 and 6 illustrate flowchart of P&O algorithm based MPPT and its block diagram model in Matlab/Simulink.

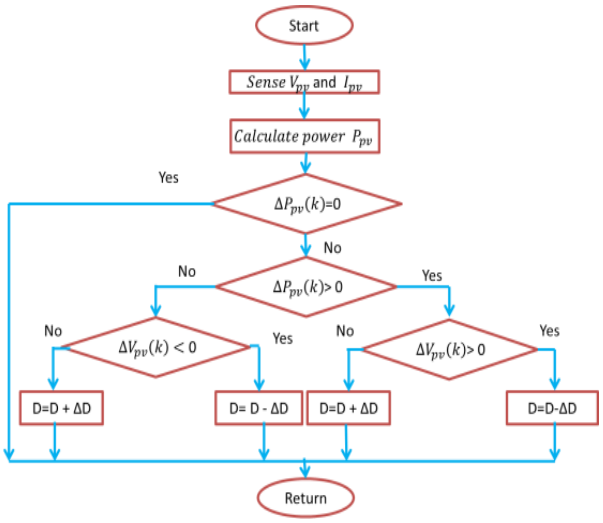

Figure 5. Flowchart of P&O algorithm based MPPT

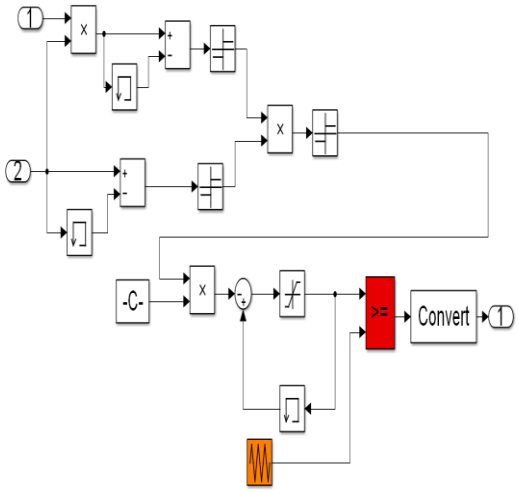

Figure 6. MPPT block diagram in Matlab/Simulink

- If **ΔP > 0** then the disturbance of the voltage moves the operating point to a point closer to the MPP and the technique continues to disturb the voltage in the same direction. It will move the operating point until reaching the MPP.
- If **ΔP < 0** the operating point moves away from the MPP then the voltage is disturbed with an algebraic sign opposite to the preceding sign to move the operating point until the MPP is reached.

3.2. IRFOC based on PI regulator

Starting with rotor speed and rotor flux tracking errors, we compute first the control laws I_{sd}^{*} and I_{sq}^{*}. The second step is to transform these signals expressed in synchrounous reference frame to stationary phase coordinate system using dq-to-abc transformation [12], [25-28]. The figure 7 illustrates the block diagram of IRFOC based on PI speed. Stator currents references are given by:

$$I_{sd}^{*} = \Psi_{ref} / M \tag{15}$$

$$I_{sq}^{*} = K_p(\omega_r - \omega_{ref}) + K_i \int (\omega_r - \omega_{ref})dt \tag{16}$$

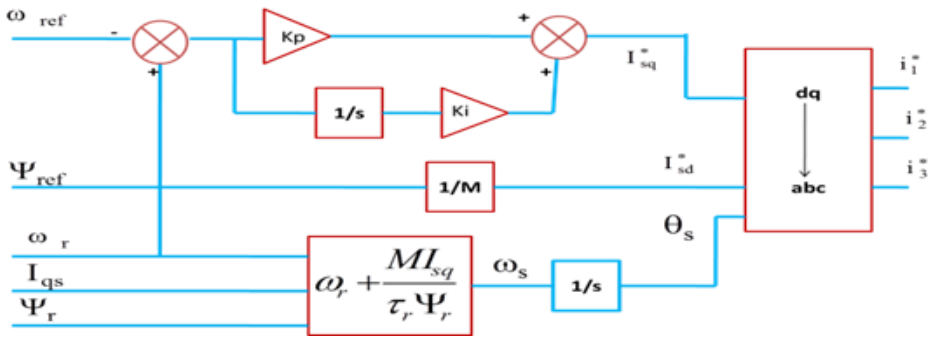

Figure 7. Block diagram of IRFOC based on PI speed regulator

4. NONLINEAR CONTROLLERS

Nonlinear controllers aim to ensure asymptotic convergence of the three outputs to be controlled.

$$\begin{cases} \lim\limits_{t\to\infty}\omega_r(t)=\omega_{ref}(t) \\ \lim\limits_{t\to\infty}\Psi_r(t)=\Psi_{ref} \\ \lim\limits_{t\to\infty}\dfrac{\partial P_{pv}}{\partial V_{pv}}=\lim\limits_{t\to\infty}\dfrac{\partial(I_{pv}V_{pv})}{\partial V_{pv}}=0 \end{cases} \quad (17)$$

Let us define

$$\varepsilon_1(t)=\frac{\partial P_{pv}}{\partial V_{pv}}=\mathrm{I_p}+V_{pv}h_0 \;\; ; \; \varepsilon_2=\omega_r-\omega_{ref} \; ; \; \varepsilon_3=\Psi_r-\Psi_{ref}; \; h_0=\frac{\partial I_{pv}}{\partial V_{pv}}; \; s_1(t)=\dot{\varepsilon}_1(t)+\lambda_1\varepsilon_1(t)$$

$$; \; \omega_{ref}(t)=\sqrt[3]{\eta_{MP}V_{mpp}I_{mpp}/K}$$

$$f=V_{pv}\frac{\partial^2 I_{pv}}{\partial^2 V_{pv}}+2\frac{\partial I_{pv}}{\partial V_{pv}} \quad ; \quad \mu(t)=-\frac{f}{C_p}\frac{V_b}{L_b} \quad \dot{f}=\dot{V}_{pv}(3h+\dot{h}); \quad h=\frac{\partial^2 I_{pv}}{\partial^2 V_{pv}}; \quad \dot{h}=V_p\frac{\partial^3 I_{pv}}{\partial^3 V_{pv}}$$

4.1. First order sliding-mode control (SMC)

The real control law u (the duty cycle of the boost converter) is formulated as [29]:

$$u=-\left(-f\frac{V_{pv}-V_b}{C_pL_b}+\frac{I_{pv}-I_L}{C_p}\left(\dot{f}+\lambda_1 f+\frac{1}{C_p}\frac{\partial I_{pv}}{\partial V_{pv}}f\right)\right)\left(-\frac{f}{C_p}\frac{V_b}{L_b}\right)-\eta_1 sign(s_1)-k_1s_1 \quad (18)$$

According to the derivative of Lyapunov function V_1, the closed loop system is asymptotically stable:

$$\dot{V}_1=s_1\dot{s}_1=-\eta_1|s_1|-k_1s_1^2 \quad (19)$$

Define the sliding surface

$$s_2(\varepsilon_2,\varepsilon_3)=s_2(\varepsilon)=\left(\frac{\partial}{\partial t}+\lambda_2\right)^{r_2-1}\varepsilon=\varepsilon \quad (20)$$

The sliding mode inverter control is expressed by:

$$\begin{bmatrix} I_{sd}^* & I_{sq}^* \end{bmatrix}=-\underbrace{\begin{bmatrix} 0 & a_1\Psi_r \\ a_7 & 0 \end{bmatrix}}_{A}^{-1}\begin{bmatrix} -\hat{a}_2-a_3\omega_r-\dfrac{d\omega_{ref}}{dt} \\ a_8\Psi_r \end{bmatrix}-\eta_2 sign(s_2)-k_2s_2 \quad (21)$$

From time derivative of second Lyapunov function, it can be seen that the closed loop system is asymptotically stable:

$$\dot{V}_2=s_2\dot{s}_2=-\eta_2|s_2|-k_2s_2^2 \quad (22)$$

4.2. Backstepping control

Let:

$$\dot{\varepsilon}_1=(V_{pv}h+2h_0)\dot{V}_{pv}=\left(\frac{I_{pv}-I_L}{C_p}\right)f; \quad \varepsilon_{10}(t)=I_L-\alpha_1$$

$$\alpha_1=(I_{pv})_{ss}=\mathrm{I_{pv}}+C_{pv}c_1\varepsilon_1/f; \quad \dot{\alpha}_1=\frac{\partial I_{pv}}{\partial V_{pv}}\dot{V}_{pv}+C_p\left(fc_1\dot{\varepsilon}_1-\dot{f}c_1\varepsilon_1\right)/f$$

The MPPT control law *u* is expressed as**[**12]:

$$u = \frac{L_b}{V_b}\left(\frac{f\varepsilon_1}{C_p} - c_2\varepsilon_{10} + \dot{\alpha}_1\right) - \frac{V_{pv}}{V_b} + 1 \tag{23}$$

The inverter control I_{sd}^* and I_{sq}^* can be given as [30]:

$$I_{sd}^* = (-c_4\varepsilon_3 - a_8\Psi_r)/a_7 \tag{24}$$

$$I_{sq}^* = \left(-c_3\varepsilon_2 + a_2 + a_3\omega_r + \frac{d\omega_{ref}}{dt}\right)/a_1\Psi_r \tag{25}$$

It is possible to demonstrate that the time derivative Lyapunouv functions are negative. Consequently, asymptotic stability of closed loop system is guaranteed.

4.3. Rotor speed and load torque estimators

Load torque disturbance and rotor speed are needed to implement the inverter control. Estimators are widely used to avoid expensive mechanical sensors and increase reliability of the overall system. These estimators are given by:

$$\hat{C}_r = a\hat{\omega}_r{}^2 \tag{26}$$

$$\frac{d\hat{\omega}_r}{dt} = a_1\Psi_r I_{sq} - a_2 - a_3\hat{\omega}_r \tag{27}$$

5. SIMULATION RESULTS

We tested the linear and nonlinear controllers by simulations using Matlab/Simulink environnement. The parameters of the suggested controllers are chosen to achieve high performance. Their sizing is based on successive test method. The design parameters of the proposed controllers are chosen as:

- PI controller: $(K_i = 5, K_p = 200)$;
- Sliding-mode: $(\eta_1 = k_1 = 9000, \lambda_1 = 1200)$, $(\eta_2 = k_2 = 3000)$;
- Backstepping: $(c_1 = 1000, c_2 = 100000, c_3 = c_4 = 3000)$.

Solar irradiation variations are chosen in two extreme cases: low irradiation of 500W/m^2 and high irradiation of 1000W/m^2. Temperature is fixed at T=298.5˚K and is increased to 323.15˚K at time t=3.5s. maximum power and voltage, rotor speed, rotor flux, load torque and switching functions are reported in Figures 8 to 13. As the simulation results show, all proposed strategies achieve the desired objectives. Linear and nonlinear control based MPPT algorithm reach maximum power and voltage delivered by the PV generator recapitulated in Table 2. IRFOC based on conventional PI speed controller, Backstepping and sliding mode force the estimated rotor speed to track the reference value calculated from the obtained MPP, and the rotor flux is kept to its desired level. Moreover, these controllers achieve decoupling between rotor flux and electromagnetic torque.

Even if, in transient state, all the controllers present a delay, they respond quickly in steady state. Sliding mode and Backstepping show the same behavior: they exhibit fast dynamic performance, stable response and have fast and better transient responses than P&O based MPPT algorithm combined with IRFOC based on PI speed controller. It can be seen also that the linear controller present oscillatory behavior around the MPP in steady state operation, around rotor speed reference and occasional deviation from the maximum operating point in case of rapidly changing atmospheric conditions especially in the third operating point. However, P&O – IRFOC based on PI speed controller have a simple structure, require only measurement of PV voltage and PV current to track the MPP and is independent on the PV generator characteristics in the MPPT technique. This technique has the advantage of simplicity that makes it the most commonly used in commercial PV system.

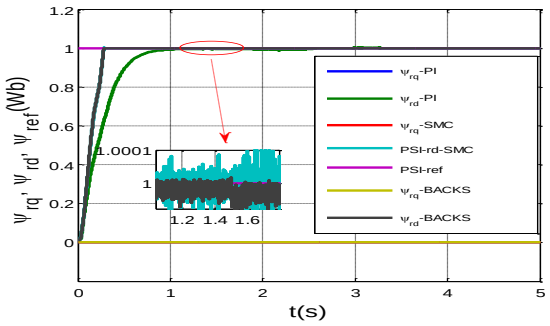

Figure 8. Rotor flux (Wb)

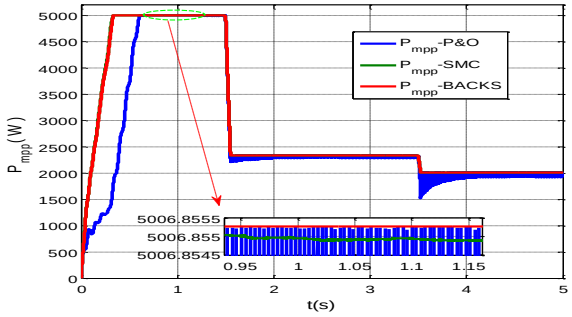

Figure 9. Maximum power (W)

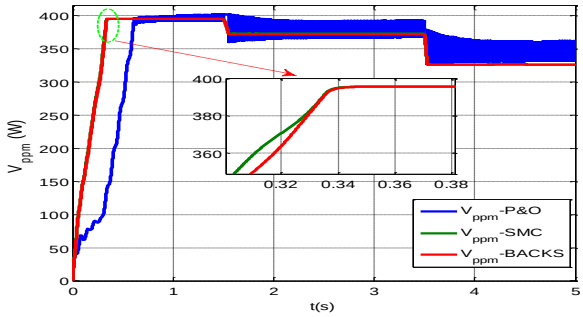

Figure 10. PV voltage

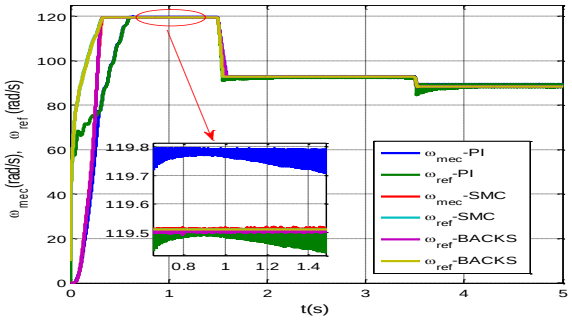

Figure 11. Rotor speed

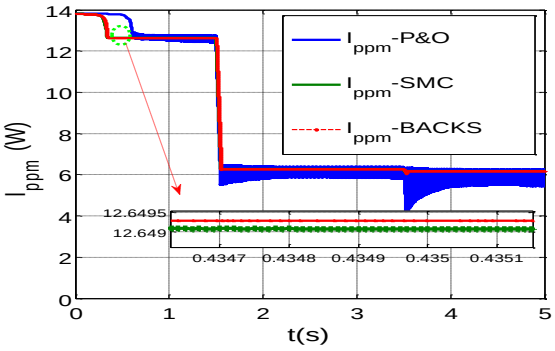

Figure 12. PV current

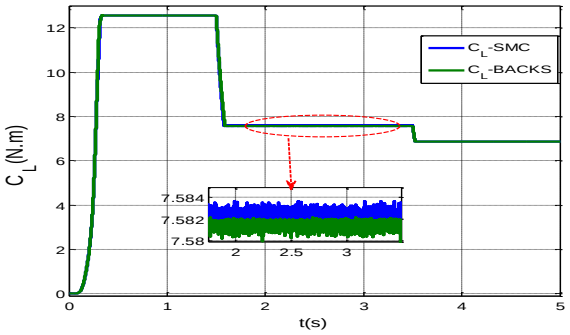

Figure 13. Load torque estimator

6. CONCLUSION

This paper introduced three control strategies for solar photovoltaic water pumping system powered by an induction motor driving a centrifugal pump. It provided a comparative study between three control strategies of a SPVWPS namely: P&O – IRFOC based on PI speed controller, Backstepping and Sliding-mode controls combined with IRFOC. Mathematical models of the main elements of the system were proposed. All the controllers reached the MPP under abrupt changing in climatic conditions and tracked accurately the desired value of rotor speed and rotor flux. Rotor speed was estimated using only the measurement of stator current, the estimate of rotor flux, mathematical model of motion equation and simple model of the centrifugal pump. An open loop estimator was proposed to estimate rotor flux. Nonlinear controller showed clearly good behavior in transient and steady state, presented fast response time and good robustness against variations of climatic conditions and less oscillation around the maximum point in the three operating points. Stability of nonlinear controller was guaranteed by means of Lyapunov analysis. In contrast, it is not possible to demonstrate stability of P&O – IRFOC based on PI speed controller. In the next work, it is possible to propose a robust non linear controller of SPVWPS using a new model of centrifugal pump replacing the classical parabolic model.

REFERENCES

[1] Omar Nait Mensour, Sahar Bouaddi, Brahim Abnay, B. Hlimi, "Mapping and Estimation of Monthly Global Solar Irradiation in Different Zones in Souss-Massa Area Morocco, Using Artificial Neural Networks," *International Journal of Photoenergy*, vol.4, pp.1-19, October 2017.

[2] Karim Choukri, Ahmed Naddami and Sanaa Hayani, "Renewable energy in emergent countries: lessons from energy transition in Morocco," Energy, Sustainability and Society, vol. 7, no. 1, December 2017

[3] Hairul Nissah Zainudin, Saad Mekhilef, "Comparison Study of Maximum Power Point Tracker Techniques for PV Systems," MEPCON'10, Cairo University, Egypt, December 2010.

[4] S. Chin, J. Gadson, and K. Nordstrom, "Maximum Power Point Tracker," *Tufts University Department of Electrical Engineering and Computer Science*, pp. 1-66., 2003.

[5] R. Faranda and S. Leva, "Energy Comparison of MPPT techniques for PV Systems," *WSES Transaction on Power Systems*, vol. 3, pp. 446-455, 2008.

[6] Moshiur Rahman Sourov, Ummee Tania Ahmed, Mirza Golam Rabbani, "A High Performance Maximum Power Point Tracker for Photovoltaic Power System Using DC-DC Boost Converter," *IOSR Journal of Engineering*, vol. 2, no. 12, pp. 12-20. Dec 2012.

[7] M.S. Aït Cheikh, C. Larbes, G.F. Tchoketch Kebir and A. Zerguerras, "Maximum power point tracking using a fuzzy logic control scheme," *Revue des Energies Renouvelables*, vol. 10, pp. 387-395, 2007.

[8] Swetapadma Panigrahi, Amarnath Thakur, "Modeling and simulation of three phases cascaded H-bridge grid-tied PV inverter," *Bulletin of Electrical Engineering and Informatics*, vol. 8, no. 1, pp. 1-9, March 2019.

[9] Rihab Mahjoub Essefi, Mansour Souissi, Hsan Hadj Abdallah, "Maximum Power Point Tracking Control Using Neural Networks for Stand-Alone Photovoltaic Systems Using Neural Networks," *International Renewable Energy Congress IREC*, pp. 1-6, 2014.

[10] H. R. Khoei and M. Zolfaghari, "New Model Reference Adaptive System Speed Observer for Field-Oriented Control Induction Motor Drives Using Neural Networks," *Bulletin of Electrical Engineering and Informatics*, vol. 5, no. 1, pp. 25-36, 2016.

[11] M'hammed Guisser, M. Aboulfatah, A. El-Jouni, Elhassane Abdelmounim, "Nonlinear MPPT controller for photovoltaic pumping system based on robust integral backstepping approach," *International Review on Modelling and Simulations*, vol. 7, no. 3, pp. 481-488, January 2014.

[12] Mhamed Madark, A. Ba-Razzouk, E. Abdelmounim, M. El Malah, "Backstepping with Integral Action Controller for a Solar Photovoltaic Powered Induction Motor," *2018 Renewable Energies, Power Systems & Green Inclusive Economy (REPS-GIE)*, Casablanca, pp. 1-6, 2018.

[13] F. Bacha, M. Gasmi, "Sliding mode control of inductionmotor-pump supplied by photovoltaic generator," *In Proceedings of IEEE International Conference on Industrial Technology*, Auburn, AL, pp. 182–187, 2011.

[14] J. Surya Kumari, Ch. Sai Babu, A. Kamalakar Babu, "Design and Analysis of P&O and IP&O MPPT Techniques for Photovoltaic System," *International Journal of Modern Engineering Research IJMER*, vol.2, no.4, pp. 2174-2180, July-Aug. 2012.

[15] M. Madark, A. Ba-Razzouk, E. Abdelmounim, M. El Malah, "Adaptive Vector Control of Induction Motor Using CTMVC," *International Review on Modelling and Simulations IREMOS*, vol. 10, no. 4, pp. 303-312, August 2017.

[16] B. Eker, "Solar Powered Water Pumping Systems," *Trakia Journal of Sciences*, vol. 3, no. 7, pp 7-11, 2005.

[17] Nahla Mohamed, Nor Zaihar Yahaya, Balbir Singh Mahinder Singh, "Single-diode model and two-diode model of PV modules: A comparison," *2013 IEEE International Conference on Control System, Computing and Engineering*, pp. 210-214, Mindeb, 2013.

[18] M. Madark, A. Ba-Razzouk, E. Abdelmounim, M. El Malah ,"An Effective Method for Rotor Time-Constant and Load Torque Estimation for High Performance Induction Motor Vector Control," *International Review on Modelling and Simulations I.RE.MO.S*, vol. 10, no. 6, pp. 410-422, December 2017.

[19] Yassine Zahraoui, Mohamed Akherraz, Chaymae Fahassa, Sara Elbadaoui , "Induction motor harmonic reduction using space vector modulation algorithm," *Bulletin of Electrical Engineering and Informatics*, vol. 9, no. 2, pp. 452-465, April 2020.

[20] Santosh S. Raghuwanshi, Vikas Khare, "Sizing and Implementation of Photovoltaic Water Pumping System for Irrigation," *IAES International Journal of Artificial Intelligence IJ-AI*, vol. 7, no. 1, pp. 54-62, March 2018.

[21] Jubaer Ahmed, Zainal Salam, "An improved perturb and observe (P&O) maximum power point tracking (MPPT) algorithm for higher efficiency," *Applied Energy*, vol 150, pp. 97-108, 15 July 2015.

[22] R. Sridhar, Dr. Jeevananathan, N. Thamizh Selvan, Saikat Banerjee, "Modeling of PV Array and Performance Enhancement by MPPT Algorithm," *International Journal of Computer Applications.* vol 7, no.5, pp. 1157-1429, 2010.

[23] E. V. Solodovnik, S. Liu, and R. A. Dougal, "Power Controller Design for Maximum Power Tracking in Solar Installations," *IEEE Transactions in Power Electronics*, vol. 19, pp. 1295-1304, Sept. 2004.

[24] I.William Christopher and Dr.R.Ramesh, "Comparative Study of P&O and InC MPPT Algorithms," *American Journal of Engineering Research AJER*, vol. 2, no. 12, pp. 402-408, 2013.

[25] A. Ba-Razzouk, A. Chériti and G. Olivier, "Artificial Neural Networks Rotor Time Constant Adaptation in Indirect Field Oriented Control Drives," *IEEE Power Electronics Specialists Conference*, Baveno, Italy, vol. 1, pp. 701-707, June 1996.

[26] A.Ba-Razzouk, A.Chériti and V.Rajagopalan, "Real-Time Implementation of a Rotor Time-Constant Online Estimation Scheme," *IECON'99. Conference Proceedings. 25th Annual Conference of the IEEE Industrial Electronics Society (Cat. No.99CH37029)*, vol. 2, pp. 927-932, November 1999.

[27] M. Zerbo, A. Ba-razzouk, P. Sicard, "Real-time Flux and Torque Estimator for Induction Machines," *IEEE Canadian Conference on Electrical and Computer Engineering CCGEI'04*, vol. 4, pp. 2159-2162, 2004.
[28] N. Kiran, "Indirect vector control of three phase induction motor using PSIM," *Bulletin of Electrical Engineering and Informatics BEEI*, vol. 3, no. 1, pp. 15-24, 2014.
[29] Mhamed Madark, A. Ba-Razzouk, E. Abdelmounim, M. El Malah, "Nonlinear Controller of Solar PV System for Water Pumping and Irrigation Applications," *2019 International Conference on Wireless Technologies, Embedded and Intelligent Systems (WITS)*, Fez, Morocco, pp. 1-6, 2019.
[30] Mhamed Madark, A.Ba-Razzouk, E.Abdelmounim, M.El Malah "A New Induction Motor Adaptive Robust Vector Control Based on Backstepping," *International Journal of Electrical and Computer Engineering IJECE*, vol. 7, no. 1, pp. 101-110, February 2017.